

Zinc-oxide-based planar nanodiodes operating at 50 MHz

Mustafa Y. Irshaid, Claudio Balocco, Yi Luo, Peng Bao, Christian Brox-Nilsen, and A. M. Song^{a)}

School of Electrical and Electronic Engineering, University of Manchester, Manchester M13 9PL, United Kingdom

(Received 9 May 2011; accepted 4 August 2011; published online 29 August 2011)

Nanometer-scale self-switching devices (SSDs) fabricated in polycrystalline zinc oxide have been demonstrated up to at least 51.5 MHz, functioning as rectifiers to generate DC voltage. The SSDs require only a single nanolithography step and hence are of interest to low-cost printed electronics. The devices showed stable performance within the frequency range tested. The as-fabricated devices possessed strongly nonlinear current-voltage characteristics, resembling those of conventional diodes. After coating the devices with poly methyl methacrylate and poly vinylidene fluoride to enhance the electric field coupling, the nonlinear behavior was maintained while the device current increased dramatically. © 2011 American Institute of Physics. [doi:10.1063/1.3629995]

The needs to fabricate electronic devices and circuits for low-cost applications such as electronic tickets, smart cards, and radio-frequency identification (RFID) tags have motivated researchers to find alternatives to the high-temperature, high-cost silicon manufacturing techniques. Low-cost RFIDs could be potentially very widely used commercially in applications such as authentication, tracking goods, or even in supermarkets for real-time monitoring of inventory and item-level tagging.¹ Printed electronics may enable these applications since it generally does not require complex lithography and/or high-temperature procedures, resulting in significant cost reductions per unit area compared to silicon-based techniques.² Despite the relatively lower performance compared to circuits based on single-crystalline silicon, research on printed electronics technologies has been progressing very rapidly in recent years and devices with carrier mobility and stability superior to amorphous-silicon thin-film transistors (TFTs) have been demonstrated.

The RF rectifier is a key component in RFID tags. Conventional diodes are either based on a doping junction or energy barrier (such as Schottky), both of multi-layered sandwich structures requiring a high degree of process control and complexity to achieve adequate RF performance by printing technologies.^{3–6} Recently, arrays of single-layered planar nano-diodes called self-switching devices (SSDs) have been fabricated by etching L- or U-shaped trenches, between which asymmetric nanochannels are formed for current to flow.^{7–9} Similar to conventional diodes, they respond differently to positive and negative voltages applied to their terminals, favoring current flow in a certain direction. Despite the diode-like characteristics, the SSD does not contain any doping junction or Schottky barrier, but relies on breaking symmetry in the nano-device geometry.⁷ Due to their planar architecture, SSDs can be fabricated in parallel arrays without interconnections, which significantly reduces parasitic elements⁸ and permits very high speed for RF and terahertz (THz) applications up to 1.5 THz.¹⁰

Polycrystalline zinc oxide (ZnO) is a low-cost, environmentally friendly semiconductor, which can be easily grown

at room- or relatively low temperatures to form thin layers by standard techniques such as magnetron sputtering,¹¹ atomic-layer deposition (ALD),¹² and pulsed-laser deposition.¹³ Transparent electronic circuits consisting of conventional TFTs have been fabricated in ZnO.¹⁴ The electron mobility is generally limited by surface roughness and carrier scatterings at grain boundaries.¹³ The room-temperature electron mobility in polycrystalline ZnO has been demonstrated to reach up to 110 cm²/Vs at elevated substrate temperature during growth.¹⁵ In most cases where ZnO is deposited onto unheated substrate, mobility is however typically below or around 1 cm²/Vs. This limits the operating frequencies of devices for RF applications. We will show here that, despite the low mobility of the ZnO material in our experiments, the greatly reduced parasitic capacitance enabled by the planar device architecture and the nanometer dimensions of the SSDs have enabled consistent RF rectification up to at least 51.5 MHz.

The samples used in this work were prepared by sputtering 40 nm of ZnO on a glass substrate, followed by fabrication of metal contacts, as shown in Fig. 1. Separate experiments to fabricate conventional TFTs using the ZnO films yielded a saturation electron mobility of 0.1 to 0.3 cm²/Vs (not shown here), which is within typical values of mobility achieved by sputter coating. No further thermal annealing treatment in oxygen was carried out, which could improve the carrier mobility but may cause an undesirable threshold voltage shift or reduction in carrier concentration. Unlike most ZnO TFTs, the operation of the SSD requires the semiconductor to be doped rather than intrinsic due to the planar layout of the active channel and ohmic contacts.⁷ The SSD contacts comprise of 120 nm of aluminum to create the ohmic contacts, and 50 nm of gold on top of the aluminum to make the contacts more distinguishable during nanolithography by electron-beam lithography (EBL). The two larger square contacts (140 μm) in Fig. 1 were included to facilitate connection to the probe stations for DC and RF measurements. The distance between the two smaller rectangular contacts (100 × 45 μm) is about 6 μm, which reduces the series resistance. A parallel array of 50 SSDs was patterned in the electron-beam resist poly methyl methacrylate (PMMA)

^{a)} Author to whom correspondence should be addressed. Electronic mail: A.Song@manchester.ac.uk.

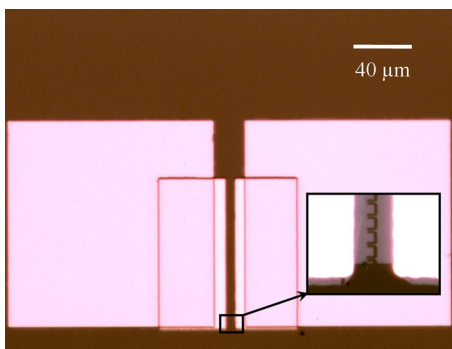


FIG. 1. (Color online) Optical microscope image of the metal contacts created by photolithography. The two large square contacts facilitate the connection to the probe stations. The inset shows a part of the parallel array of 50 SSDs.

using EBL. The nano-trenches into ZnO were then obtained by wet chemical etching using a cooled diluted solution of acetic acid (8 °C, 0.02% in deionized water). In Fig. 2, a typical atomic-force microscopy (AFM) performed on a few SSDs from the longer array shows a channel width of around 380 nm. The trenches were etched 40 nm deep sufficient to reach the substrate. Aluminum contacts were placed on the left and right sides of the SSD channels (not shown in Fig. 2 due to the scale but shown in Fig. 1). When a negative voltage is applied to left contact, the negative charges around the horizontal insulating trenches deplete the nanochannel between them, hence resulting in only a low or even zero current flow through the channel. In contrast, when a positive voltage is applied to the left contact, the positive charges around the trenches attract electrons into the nanochannel by field effect, which enables a high current flow. This self-switching mechanism leads to diode-like electrical behavior.⁷ In order to increase the operating speed of the devices, capacitive coupling between the left and right contacts should be reduced by increasing the width of the vertical trenches,¹⁶ which was achieved by exposing two parallel lines during EBL. The vertical trenches are hence wider than the horizontal ones in Fig. 2. The channel width was selected after experimenting with a

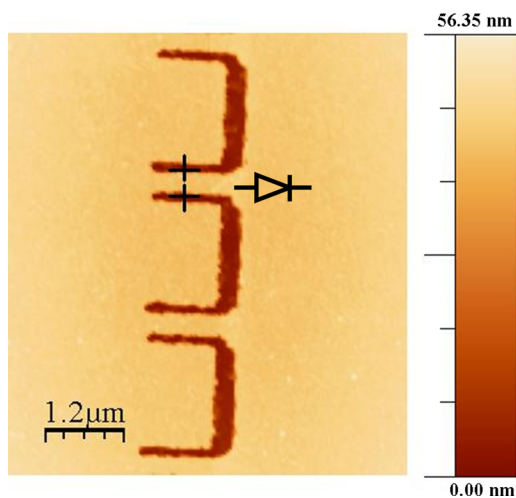


FIG. 2. (Color online) AFM image of a few SSDs from a longer parallel array of 50. The section across the channel between the two crosses measures 380 nm, with a trench depth of 40 nm reaching the substrate. The direction of the equivalent diode is shown for one SSD.

series of different channel widths. Narrower channels tend to have more nonlinear current-voltage behavior, but also lower output current in the forward direction and higher threshold voltage. Wider channels can have zero threshold voltage and result in higher output current, but suffer from increased reverse current,⁷ which is less favorable for the intended application of rectifying AC signals.

Figure 3(a) shows the nonlinear DC characteristics of the as-fabricated SSD array before coating with any encapsulating dielectric material, resembling that of conventional diodes. In the forward direction, a current of 20 nA was produced from a 10 V supply, whereas less than a tenth of that was produced in the reverse direction. The inset in Fig. 3(a) shows the rectified current produced from a sinusoidal voltage supply of 4 V (RMS value), deduced from the DC current-voltage characteristics and shown for one complete cycle. It is obvious how the behavior of the devices resembles that of a diode, producing a half-wave rectified current in response to a sinusoidal input voltage.

By spin-coating a high-k dielectric material onto the SSDs to fill in the etched trenches and also to provide a top dielectric layer, the transverse electric field coupling can be significantly enhanced, enabling a higher degree of control over opening and closing the channel.¹⁷ As a result, the channel conductance is increased and the output current is higher under the forward-bias condition. Spin-coating PMMA and poly vinylidene fluoride (PVDF) followed by quenching in water have been demonstrated to achieve a dielectric constant of 10 or more.¹⁸ In our experiments, the devices were coated with a 150 nm layer of PMMA followed by 130 nm of PVDF, and this resulted in a forward current

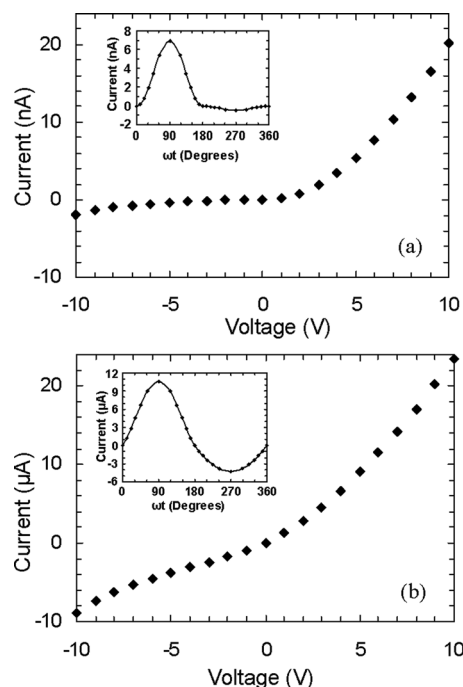


FIG. 3. DC measurement results: (a) The devices show strongly nonlinear I-V characteristics before being coated with any dielectric material. (b) After coating the devices with PMMA and PVDF layers, the devices maintained nonlinear behavior and the current increased by about three orders of magnitude. The insets in the two graphs show the half-wave rectified currents deduced from the DC characteristics for one complete cycle of a sinusoidal voltage supply of 4 V RMS.

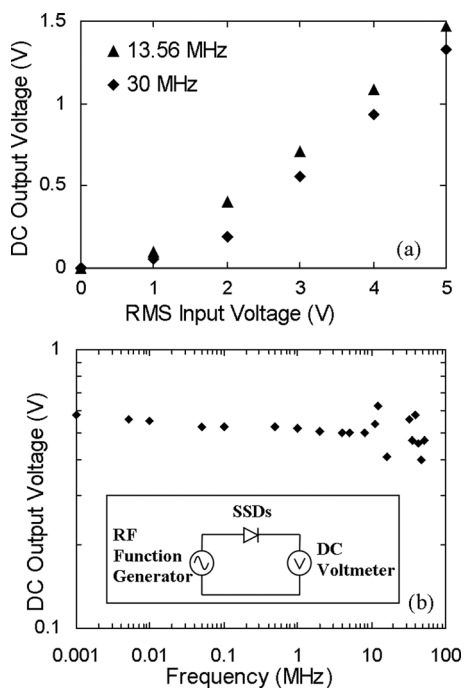


FIG. 4. (a) The response of the SSDs to a varying sinusoidal input voltage at 13.56 and 30 MHz. (b) The rectified DC output of the SSDs as a function of RF frequency up to 51.5 MHz. The inset in (b) shows the setup used to obtain these results.

about three orders of magnitude larger at 10 V than the uncoated case, as seen in Fig. 3(b). Although the reverse current also increased after coating ($<9 \mu\text{A}$), it is still much lower than the forward current ($23 \mu\text{A}$) and the devices maintained nonlinear behavior, which allowed rectification of RF signals. Apart from the enhanced electric field coupling, the dramatically increased current might also be due to the passivation of the ZnO surface electron traps and isolation from oxygen and hydroxyl groups as barrier layers. The inset in Fig. 3(b) shows the current produced from a sinusoidal voltage supply of 4 V (RMS value), deduced from the DC current-voltage characteristics and shown for one complete cycle. The negative half cycle is smaller than the positive one, which is enough to generate a net positive DC output current.

To characterize the frequency response of the fabricated devices, the setup shown in the inset of Fig. 4(b) was used, where an RF function generator provided a sinusoidal input voltage. Figure 4(a) shows how the DC output voltage of the SSDs changed with the RMS value of the input sinusoidal voltage at 13.56 and 30 MHz. At low inputs (below 1 V RMS), the output was very weak, as a result of the relatively poor nonlinearity in the DC characteristics near zero volts (Fig. 3(b)). However, above 1 V RMS, the nonlinear component becomes more significant and the DC output increased more rapidly indicating better rectification. The non-zero reverse current appearing in Fig. 3(b) certainly reduced the DC output. Optimization on channel width and/or ZnO mate-

rial properties shall allow significant improvements. Figure 4(b) shows the RF measurement results of the SSDs up to 51.5 MHz. The output remained rather consistent and varied within 3 dB range for all frequency values up to the maximum frequency provided by the function generator. The more scattered data points at higher frequencies were most likely due to resonances induced by the long coaxial cables used in our experiments. The fairly stable output suggests that the operating frequency range actually extends beyond 51.5 MHz.

In conclusion, we have shown that nanometer-scale SSDs fabricated in low-cost poly crystalline ZnO semiconductor have rectified RF signals up to at least 51.5 MHz. Although the fabrication was carried out by EBL in this work, the single-layered device architecture makes it ideal to use nano-imprint technique as previously demonstrated using organic semiconductors.^{19,20} The device performance could well be extended to the so-called UHF frequency range from hundreds of MHz to a few GHz, if ZnO films with higher mobilities are used.

¹C. J. Drury, C. M. J. Mutsaers, C. M. Hart, M. Matters, and D. M. de Leeuw, *Appl. Phys. Lett.* **73**, 108 (1998).

²V. Subramanian, J. M. J. Fréchet, P. C. Chang, D. C. Huang, J. B. Lee, S. E. Molesa, A. R. Murphy, D. R. Redinger, and S. K. Volkman, *Proc. IEEE* **93**, 1330 (2005).

³V. Subramanian, P. C. Chang, J. B. Lee, S. E. Molesa, and S. K. Volkman, *IEEE Trans. Compon., Packag. Technol.* **28**, 742 (2005).

⁴S. Steudel, K. Myny, V. Arkhipov, C. Deibel, S. De Vusser, J. Genoe, and P. Heremans, *Nature Mater.* **4**, 597 (2005).

⁵S. Steudel, S. D. Vusser, K. Myny, M. Lenes, J. Genoe, and P. Heremans, *J. Appl. Phys.* **99**, 114519 (2006).

⁶J. Sun, B. N. Pal, B. J. Jung, and H. E. Katz, *Org. Electron.* **10**, 1 (2009).

⁷A. M. Song, M. Missous, P. Omling, A. R. Peaker, L. Samuelson, and W. Seifert, *Appl. Phys. Lett.* **83**, 1881 (2003).

⁸C. Balocco, H. Halsall, N. Q. Vinh, and A. M. Song, *J. Phys.: Condens. Matter* **20**, 384203 (2008).

⁹C. Balocco, A. M. Song, M. Åberg, A. Forchel, T. González, J. Mateos, I. Maximov, M. Missous, A. A. Rezazadeh, J. Saijets, L. Samuelson, D. Wallin, K. Williams, L. Worschech, and H. Q. Xu, *Nano Lett.* **5**, 1423 (2005).

¹⁰C. Balocco, S. R. Kasjoo, X. F. Lu, L. Q. Zhang, Y. Alimi, S. Winnerl, and A. M. Song, *Appl. Phys. Lett.* **98**, 223501 (2011).

¹¹E. Fortunato, P. Barquinha, A. Pimentel, A. Gonçalves, A. Marques, R. Martins, and L. Pereira, *Appl. Phys. Lett.* **85**, 2541 (2004).

¹²A. Yamada, B. Sang, and M. Konagai, *Appl. Surf. Sci.* **112**, 216 (1997).

¹³K. Ellmer, *J. Phys. D: Appl. Phys.* **34**, 3097 (2001).

¹⁴D. Zhao, D. A. Mourey, and T. N. Jackson, *IEEE Electron Dev. Lett.* **31**, 323 (2010).

¹⁵B. Bayraktaroglu, K. Leedy, and R. Neidhard, *IEEE Electron Dev. Lett.* **29**, 1024 (2008).

¹⁶X. F. Lu, K. Y. Xu, G. Wang, and A. M. Song, *Mater. Sci. Semicond. Process.* **11**, 407 (2008).

¹⁷K. Y. Xu, X. F. Lu, A. M. Song, and G. Wang, *J. Appl. Phys.* **103**, 113708 (2008).

¹⁸Q. Meng, W. Li, Y. Zheng, and Z. Zhang, *J. Appl. Polym. Sci.* **116**, 2674 (2010).

¹⁹J. Kettle, S. Whitelegg, A. M. Song, M. B. Madec, S. Yeates, M. L. Turner, L. Kotacka, and V. Kolarik, *J. Vac. Sci. Technol. B* **27**, 2801 (2009).

²⁰J. Kettle, S. Whitelegg, A. M. Song, D. C. Wedge, L. Kotacka, V. Kolarik, M. B. Madec, S. G. Yeates, and M. L. Turner, *Nanotechnology* **21**, 075301 (2010).